Proceedings of the International Symposium on Engineering Lessons Learned from
the 2011 Great East Japan Earthquake, March 1-4, 2012, Tokyo, Japan

CFD ANALYSIS OF BRIDGE DECK FAILURE DUE TO TSUNAMI

Jeremy D. BRICKER[1], Kazuhiko KAWASHIMA[2], and Akihiko NAKAYAMA[3]

[1] Visiting Associate Professor, Department of Civil Engineering, Tokyo Institute of Technology, Tokyo, Japan, Jeremy.bricker@gmail.com
[2] Professor, Department of Civil Engineering, Tokyo Institute of Technology, Tokyo, Japan, kawashima.k.ae@m.titech.ac.jp
[3] Professor, Department of Civil Engineering, Kobe University, Kobe, Japan, nakayama@kobe-u.ac.jp

ABSTRACT: The Tsunami resulting from the Great East Japan Earthquake caused failure of many bridges in Miyagi and Iwate Prefectures. Field surveys and numerical modeling were carried out to evaluate possible mechanisms of failure of these bridges. The OpenFOAM Computational Fluid Dynamics package was used to determine the effects of lift, drag, and moment on a typical bridge deck based on two-dimensional Reynolds-averaged simulations. Results show that deck inclination, flow speed, trapped air, entrained sediment, and tsunami surge all contribute to deck failure.

Key Words: Tsunami, bridge deck, lift, moment, CFD, surge, trapped air, inclination

INTRODUCTION

The Tsunami resulting from the Great East Japan Earthquake of March 11, 2011 caused failure of many bridges along the coast in Iwate and Miyagi Prefectures. Field surveys and numerical modeling were carried out to evaluate the mechanisms of failure of a typical bridge, using the Utatsu highway bridge in Minamisanriku town, Miyagi Prefecture (Figures 1 and 2) as a model for structure scale and shape.

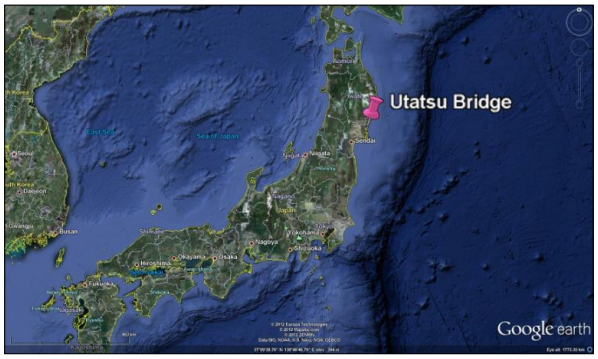

Figure 1. Google Earth map of Japan, with the location of the Utatsu Bridge indicated.

The Utatsu highway bridge was a concrete girder bridge about 8 m above water level, spanning a fishing port and river mouth. Due to the horizontal curve in the highway at this location, the bridge deck was inclined up to 3° (seaward side upward). In order to prevent deck displacement, unseating prevention devices (UPD's) were installed between girders (Figures 3 and 4).

A field survey after the tsunami showed that despite the UPD's, the inclined sections of the bridge

deck were lifted off their piers and deposited landward of the bridge in an inverted position (Figure 2, decks C, D, and E). The bridge piers and UPD's themselves incurred almost no damage (Figure 4), indicating that these deck sections experienced a large lift force or/and overturning moment. In another location, level sections of bridge deck whose UPD's were destroyed were deposited landward of the bridge in an upright position (Figure 2, decks F, G, H, I, and J), indicating they were pushed off the bridge by the drag force resulting from the flow, but this could not have been the case for the sections with undamaged UPD's.

Figure 2. Google Earth image of the Utatsu Bridge on April 6, 2011. Place-marks enumerate individual deck segments.

Figure 3. Photo of Utatsu Bridge east abutment (east end of deck A) showing steel and concrete unseating prevention devices (UPD's).

Figure 4. Photo of Utatsu Bridge pier cap between decks B (intact) and C (failed), showing intact unseating prevention devices (UPD's).

Lifting or overturning of the inclined deck sections could be a result of either (or a combination of)

hydrostatic forces (buoyancy of the deck enhanced by air trapped between the girders; i.e. Chen et al, 2005) or hydrodynamic forces (lifting or overturning of the deck like an airfoil; i.e. Kerenyi et al, 2009, and Patil et al, 2009). The OpenFOAM (2011) Computational Fluid Dynamics (CFD) package was used to determine the effects of buoyancy, lift, drag, and moment on such a bridge deck based on two-dimensional Reynolds-averaged simulations. Results show that deck inclination, flow speed, trapped air, tsunami impact, and entrained sediment could all contribute to deck failure.

TSUNAMI BEHAVOIR

In Tohoku, two types of tsunami behavior were observed. In regions of shallow offshore bathymetry (such as southern Miyagi Prefecture), the tsunami approached shore as a surge or bore (a turbulent wall of water). In areas with deeper offshore bathymetry, such as Iwate and northern Miyagi Prefectures, the tsunami appeared as a smoothly rising water surface. This paper investigates both of these situations.

Based on video taken by a local resident, the tsunami at Utatsu can be seen rising gradually, though the instant when the water submerged the bridge deck is not captured on the video. Flow near the bridge appears subcritical in the video, with a speed between 3 m/s and 5 m/s based on visual tracking of floating debris. The following simulations are based on these flow speeds.

MODEL SETUP

Fluid forces on the model bridge deck were evaluated using the OpenFOAM (Open source Field Operation And Manipulation) computational fluid dynamics (CFD) software. Simulation was carried out using a two-dimensional grid. Figure 5 shows detail of the grid near the bridge. The full domain spans 110 m in the horizontal and either 20 m (for rising free surface simulations) or 30 m (for surge and steady flow simulations) in the vertical. The bridge itself is inclined 3° upward on the seaward (left) side. Bridge deck width is 7.9 m and deck thickness is 0.5 m. Girder height is 2 m and girder thickness is 0.6 m, spaced 1.9 m on center. Curbs on the edges of the deck are 0.2 m tall by 0.4 m wide. The landward edge of the landward girder is located 8 m above the ground.

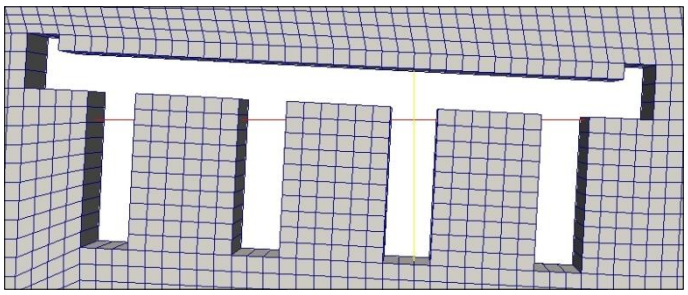

Figure 5. Detail of OpenFOAM mesh near the Utatsu Bridge.

Grid cell size is 0.2 m x 0.2 m on average, though this varies slightly due to non-orthogonality introduced by the inclined bridge (the grid follows the surface of the bridge as well as the model domain boundaries, so non-orthogonality is introduced because these surfaces are oblique to each other). Boundary conditions used in the simulations are shown in Table 1.

The model was run as a Reynolds Averaged Navier Stokes (RANS) simulation, using the standard k-ε turbulence closure model. Within OpenFOAM, the interFOAM module was used, in order to simulate two-phase (air and water) flow. The PIMPLE (merged PISO/SIMPLE) algorithm was used for transient Navier-Stokes solution. Interface compression (anti-diffusion) was enacted in order to maintain a sharp air-water interface. An iterative correction for grid non-orthogonality was also

activated to enhance model stability and accuracy. The model time step was variable, to keep the Courant number below 0.5. Typically, this resulted in a time step between 0.001 sec and 0.01 sec.

Table 1. Boundary and initial conditions used in the OpenFOAM model.

Location	Boundary Condition for surge simulation	Boundary Condition for rising surface and steady simulations
Ground (bottom surface) and Bridge	No-slip, with physical roughness height 1 mm	No-slip, with physical roughness height 1 mm
Atmosphere (upper surface)	Constant pressure (atmospheric)	Constant pressure (atmospheric)
Inlet (left surface)	Constant (specified) water level; velocity calculated from pressure gradient	Time-varying (specified) water level; constant (specified) velocity
Outlet (right surface)	Outflow	Outflow
Initial condition	Specified water surface and flow velocity	Specified water surface and flow velocity

MODEL SCENARIOS

The model was run to investigate two situations, both of which were experienced by bridges in Tohoku:

1. The bridge is struck by a tsunami surge (i.e., southern Miyagi Prefecture).
2. The bridge is engulfed by a smoothly rising water surface (as was the case at Utatsu).

Boundary conditions are detailed in Table 1, and example time series for both cases are shown in Figures 6 and 7.

As Figure 6 shows, the surge scenario is not the case of a turbulent bore (a wall of water) impacting the structure; rather, it is the case of a sloping water surface surging into the structure. The surge begins as a 3-m high step in the free surface located 10 m upstream of the bridge, but relaxes into the sloping surface shown before impacting the bridge.

Baseline surge simulations were run with a water density of 1030 kg/m^3, which represents seawater. As a conservative sensitivity analysis, additional simulations were run with a water density of 1200 kg/m^3, which assumes that 10% of the flow volume consisted of entrained sediment and debris (Applied Technology Council, 2008).

Simulations assumed that the air which became trapped between girders could not escape upward (air trapped between girders is visible in Figures 6 and 7). Furthermore, air was assumed to be incompressible, which is a conservative assumption, as in reality trapped air would be compressed and thus occupy a smaller volume (and cause less buoyancy) than here modeled.

Video of the tsunami indicates the water level rose 3 m to 4 m above the bridge deck elevation, and the flow appears to have been subcritical, meaning the flow speed was less than 12 m/s for an approximately 15 m deep flood. Simulations were thus carried out for initial flow speeds of 3 m/s, 5 m/s, 7 m/s, and 9 m/s.

As a final sensitivity analysis, the above cases were also analyzed for the case of a level bridge deck. This is to determine what effect the 3° deck inclination had on the deck failure. For the level bridge deck simulations, the grid of Figure 5 was modified to remove the bridge inclination, resulting in an orthogonal grid for these simulations.

In addition to the surge simulations, smoothly rising surface simulations (Figure 7) were carried out with the initial free surface located 8 m above ground level (at the bottom of the bridge girders), then rising up to a maximum elevation of 15 m above ground level (4 m above the bridge deck). However, due to an upstream instability (Figure 7, t=801 sec) in the rising surface simulation for water levels higher than approximately 12 m above ground (1 m above the bridge deck), a separate steady-state simulation was carried out for the case of a water level of 15 m above ground (4 m above

the bridge deck), for each horizontal flow speed case. An example of this steady-state simulation is shown in Figure 8, after 29 sec of spin-up from an initial condition of a level free surface and uniform flow speed.

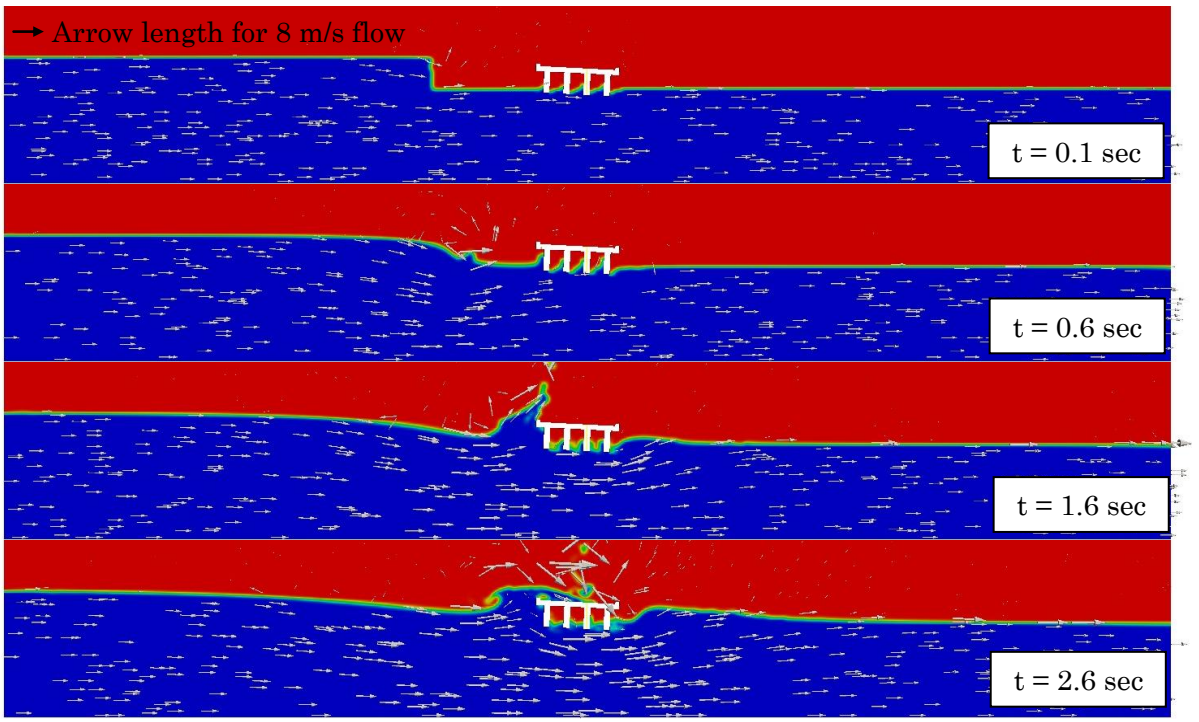

Figure 6. Phase (blue=water and red=air) and flow velocity for the bridge being submerged by a tsunami surge. For this case, initial flow speed is 3 m/s, and water density is 1030 kg/m^3.

RESULTS

Calculation of forces

Pressure along the bridge surface (Figure 9) was extracted from the model runs in order to calculate lift, drag, and moment on the bridge deck under all scenarios. These quantities were calculated via equations (1) – (4):

$$\vec{F}_k = P_k \, dw_k \, \hat{n}_k \quad (1)$$

$$F_{drag} = \sum \vec{F}_k \cdot \hat{\imath} \quad (2)$$

$$F_{lift} = \sum \vec{F}_k \cdot \hat{\jmath} \quad (3)$$

$$M_{overturning} = -\sum \vec{r}_k \times \vec{F}_k \quad (4)$$

in which $\vec{F}_k$: force per unit length of bridge acting on the k^{th} cell along the deck surface, P_k: pressure acting on the k^{th} cell along the deck surface, dw_k: width of the k^{th} cell along the deck surface, $\hat{n}_k$: unit vector normal to the k^{th} cell along the deck surface, F_{drag}: total drag force per unit length acting on the bridge deck, $\hat{\imath}$: horizontal unit vector, F_{lift}: total lift force per unit length acting on the bridge deck, $\hat{\jmath}$: vertical unit vector, $M_{overturning}$: overturning moment per unit length acting about the bottom of the landward-most girder, and $\vec{r}_k$: vector pointing from the bottom of the landward-most girder to the k^{th} cell along the deck surface.

To determine whether the bridge deck would be displaced by the lift or moment that it is exposed

to, the bridge's weight per unit length was calculated assuming a density of 2600 kg/m^3, which is standard for concrete. The Utatsu Bridge has a cross-sectional (concrete) area of approximately 8.91 m^2, resulting in a weight per unit bridge length of 227 kN/m and a restoring moment per unit bridge length about the landward girder of 716 kNm/m.

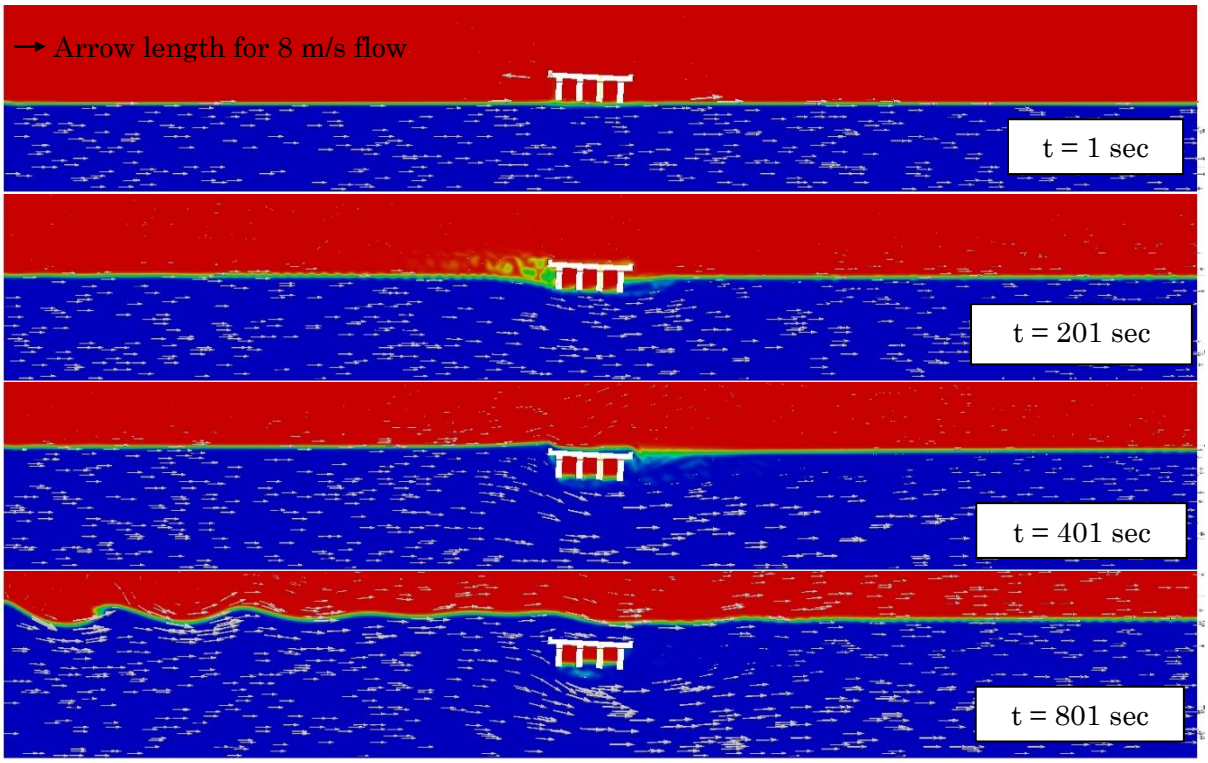

Figure 7. Phase (blue=water and red=air) and flow velocity for the bridge being engulfed by a rising water surface with ambient flow speed 3 m/s. Water density is 1030 kg/m^3.

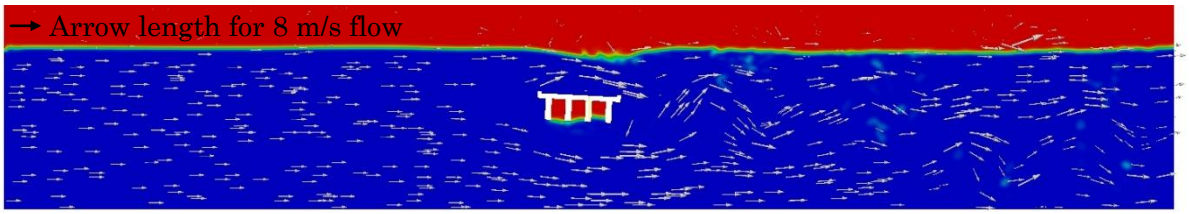

Figure 8. Phase (blue=water and red=air) and flow velocity vectors at t=29 sec for the bridge subject to steady flow of speed 3 m/s and depth 15 m. Water density is 1200 kg/m^3.

Example timeseries of forces

Figure 10 shows a time series of total lift, drag, and moment for the example case corresponding to the flow shown in Figure 6 (surge case, inclined deck, flow density 1030 kg/m^3, flow speed 3 m/s). For the first 2 seconds of the simulation, lift and moment are both positive, as the approaching flow surges up against the seaward side of the bridge deck. At t=1.1 sec, the moment is even large enough to overcome the bridge's weight and cause the deck to tilt upward on the landward side and begin to overturn. After t=2.6 sec, the wave which had surged up above the bridge deck, now comes crashing down onto the top of the deck, causing a negative lift and moment.

Figure 11 shows a similar timeseries of forces, corresponding to the flow shown in Figure 7 (rising surface case, inclined deck, flow density 1030 kg/m^3, flow speed 3 m/s). At t=0, flow begins

with a level free surface. However, the bridge acts as an obstacle to the flow and has two effects. One effect is that the flow under the bridge accelerates, lowering the pressure under the bridge and causing a negative lift and moment. This effect continues throughout the simulation period. The second effect is that the rising free surface causes a gradual increase in lift and moment due to buoyancy of the bridge (the static buoyant force on the deck including the effect of incompressible air completely filling the spaces between girders is 169 kN/m, and the overturning moment due to this buoyancy is 532 kNm/m). After submergence, the lift and moment due to buoyancy remain relatively constant, while the accelerated flow under the bridge continues to hold the deck down. Toward the end of the simulation, lift and moment both begin to increase again, as the higher water level allows more flow to pass over the bridge; this reduces the negative lift compared to that experienced at lower water levels when all the flow had to pass (and accelerate) under the bridge.

Figure 12 shows a timeseries of forces corresponding to the steady flow simulation of Figure 8 (inclined deck, flow density 1200 kg/m^3, flow speed 3 m/s). The first few seconds of this simulation can be considered a spin-up from initial conditions of uniform flow and a level free surface. At t=16-17 sec and t=28-30 sec, the overturning moment is large enough to displace the deck.

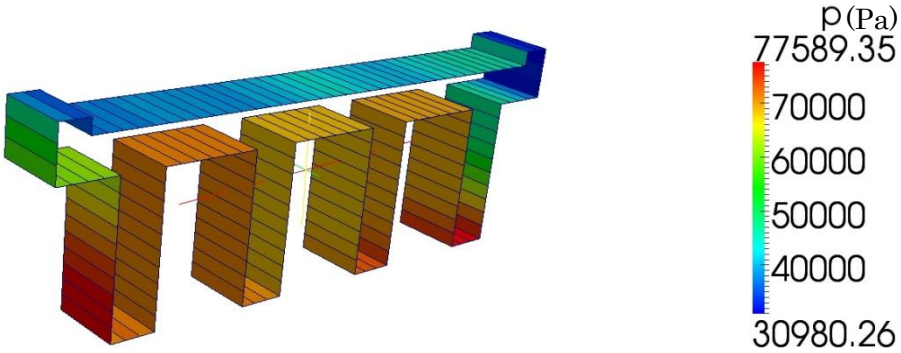

Figure 9. Example of pressure calculated by OpenFOAM on each cell along the bridge deck section surface, at 29 sec into the simulation of the "steady, 3 m/s, inclined deck, water density 1200 kg/m^3" case (Figure 8). The deck section is shown skewed for clarity of the colors on the surface.

Mechanisms causing deck failure

Deck failure can be a result of both lift force and overturning moment. These processes work together to cause failure, but they are analyzed separately here for simplicity. In the following results, failure due to overturning moment is much more readily achieved than failure due to lift force alone.

Lift

Figures 13 and 14 show the maximum (in time) lift force and overturning moment on the bridge deck for each simulation. Figure 13 shows the lift force for the smoothly rising surface and steady flow cases simulated is never large enough to cause deck failure via upward translation.

The surge simulations in Figure 13 show that at initial flow speeds greater than about 6 m/s, a tsunami surge generates enough lift to cause failure of the inclined bridge deck. The level bridge deck, however, does not fail due to lift alone at any speed. This shows that the bridge deck inclination angle has a substantial effect on the stability of the deck during tsunami surge; a deck inclined on the seaward side experiences substantially more lift than a level deck does.

Figure 13 also shows that the density of water has a significant effect on lift force during the surge simulations. Turbid flow with specific gravity (SG) of 1.2 generates more lift than standard seawater (SG=1.03) does. However, this effect is secondary to the effect of the inclined deck in the surge cases investigated.

Another item that has a substantial effect on lift is trapped air. However, it does not add enough lift to overcome the weight of the bridge for any of the rising surface or steady flow cases investigated. For the surge cases, trapped air could have been responsible for pushing the lift force above that

required to move the deck. At an initial flow speed of 7 m/s, for example, the lift force for the "surge, SG=1.03, inclined" case is about 30 kN/m greater than the weight of the deck. If trapped air were allowed to escape, however, the lift force could decrease by as much as 79 kN/m (this is the static buoyant force due to incompressible air completely filling the spaces between girders). In this case, removal of trapped air could reduce the lift force to a magnitude below that which would cause deck failure.

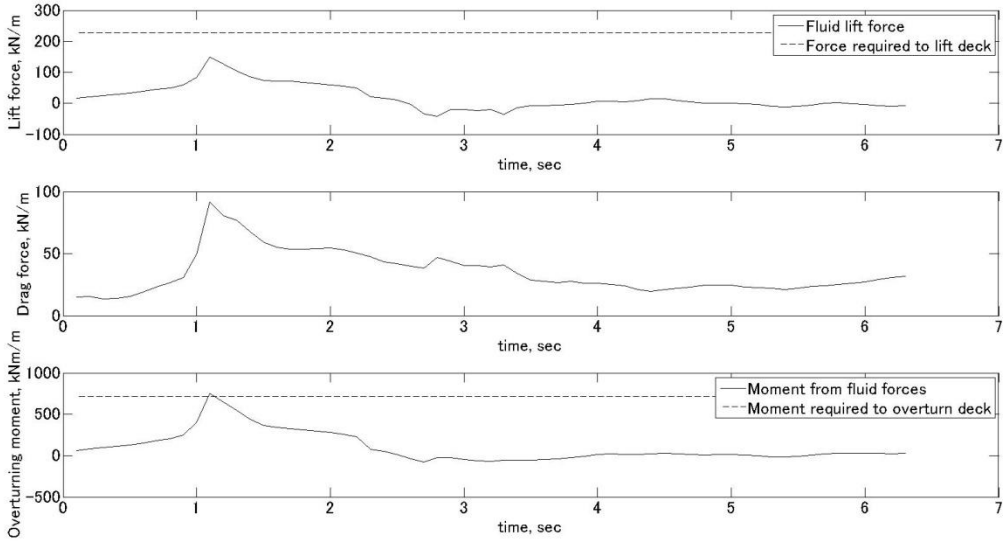

Figure 10. Example time series of fluid forces on bridge deck for the bridge being impacted by a tsunami surge. For this case, initial flow speed is 3 m/s, and water density is 1030 kg/m^3. This corresponds to the flow shown in Figure 6.

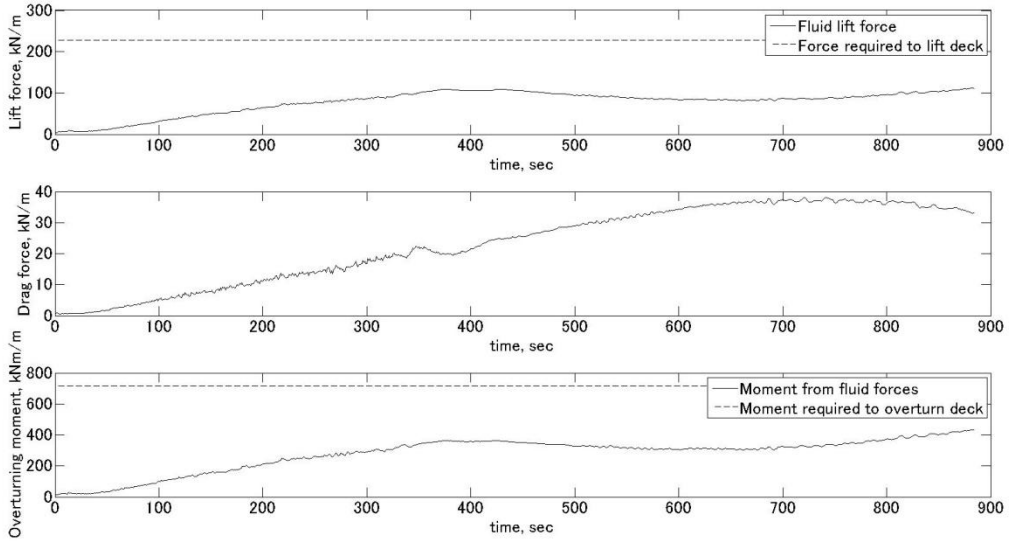

Figure 11. Example time series of fluid forces on bridge deck for the bridge subject to a smoothly rising free surface with ambient speed 3 m/s. Water density is 1030 kg/m^3. This corresponds to the flow shown in Figure 7.

Moment

Figure 14 shows that a smoothly rising surface at subcritical flow speeds does not cause a large

enough overturning moment to cause bridge deck failure (these simulations are valid for flow depths up to about 12 m). The steady flow simulations with flow depth 15 m (4 m above the bridge deck), however, cause inclined deck overturning failure for the seawater case (SG=1.03) at a flow speed of 9 m/s.

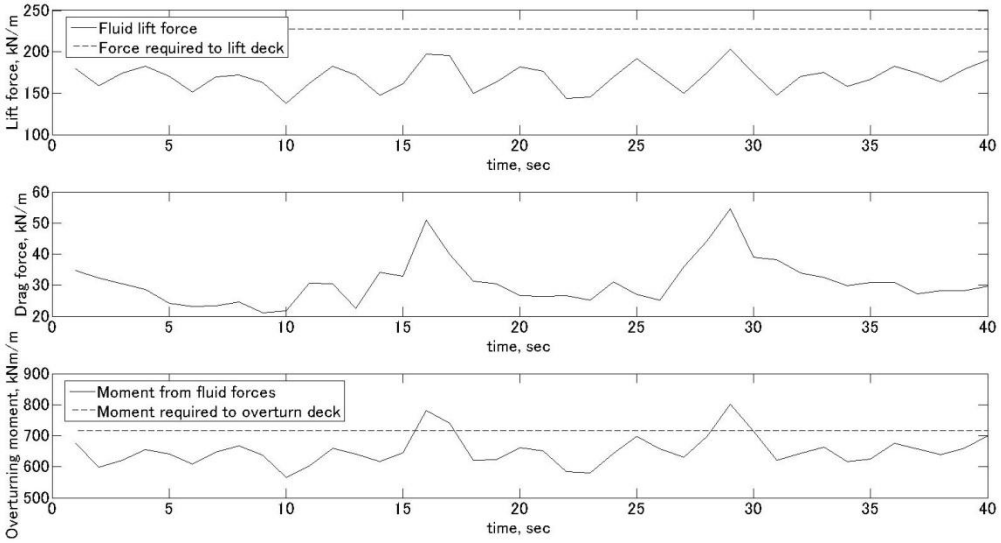

Figure 12. Example time series of fluid forces on bridge deck for the bridge subject to a free surface of elevation 15 m and speed 3 m/s. Water density is 1200 kg/m^3. This corresponds to the steady flow case shown in Figure 8.

For the turbid water (SG=1.2) case, steady flow causes inclined deck failure for flow of 3 m/s, which is close to that seen in the video from Utatsu. Figure 8 shows that for this case, the free surface experiences a slight dip over the bridge, as is expected for subcritical flow over an obstacle. Figure 9 shows the pressure distribution along the surface of the bridge deck at the time of greatest overturning moment (t=29 sec in the timeseries of Figure 12). Vortex shedding in the lee of the bridge deck is apparent in Figure 15. Vortex shedding, together with migration of the dip in the free surface over the deck, cause fluctuations in the overturning moment experienced by the deck.

To explain vortex shedding, the Strouhal number $S=nL/U$ where n is the frequency of vortex shedding, L is the length scale of the bridge deck, and U is the mean flow speed. For a cylinder in a flow, it's known that S=0.21 for a wide range of Reynolds numbers (Kundu, 1990). In the case of the bridge deck of height L=2.7 m in a flow of speed U=3 m/s, the resulting rate of vortex shedding is n=0.23 cycles/sec, which corresponds to a shedding period of about 4 sec, as is seen to be the period of the lift and moment signals in Figure 12. At speeds higher than 3 m/s, vortex shedding from the deck is replaced with a turbulent wake. Without the fluctuations of vortex shedding, maximum lift and moment at speeds higher than 3 m/s are reduced. At near-critical speeds (i.e., 9 m/s), however, overturning moment again increases, this time due to the behavior of the free surface downstream of the deck, where critical flow and a hydraulic jump periodically exist.

Unlike the steady flow cases, the surge cases induce a large enough overturning moment to cause failure of the inclined deck at all speeds modeled (3 m/s and greater). The presence of air trapped between girders is essential to inclined deck failure at low initial flow speeds though, as the static overturning moment due to air occupying the full space between girders is 248 kNm/m. Without air trapped between girders, the inclined deck (with SG=1.03) could have been stable for flow speeds up to 5 m/s, and the level deck up to 7 m/s. For the steady-flow scenarios, removal of trapped air would have prevented deck instability in all cases.

Figure 14 shows that for all scenarios, deck inclination is important in causing deck failure. The inclined deck is unstable at surge-case flows as slow as 3 m/s, while the level deck is stable at flows up

to 5 m/s. In the turbid (SG=1.2) steady-flow scenarios, the inclined deck fails at 3 m/s flow speed, while the level deck is marginally stable at this flow speed.

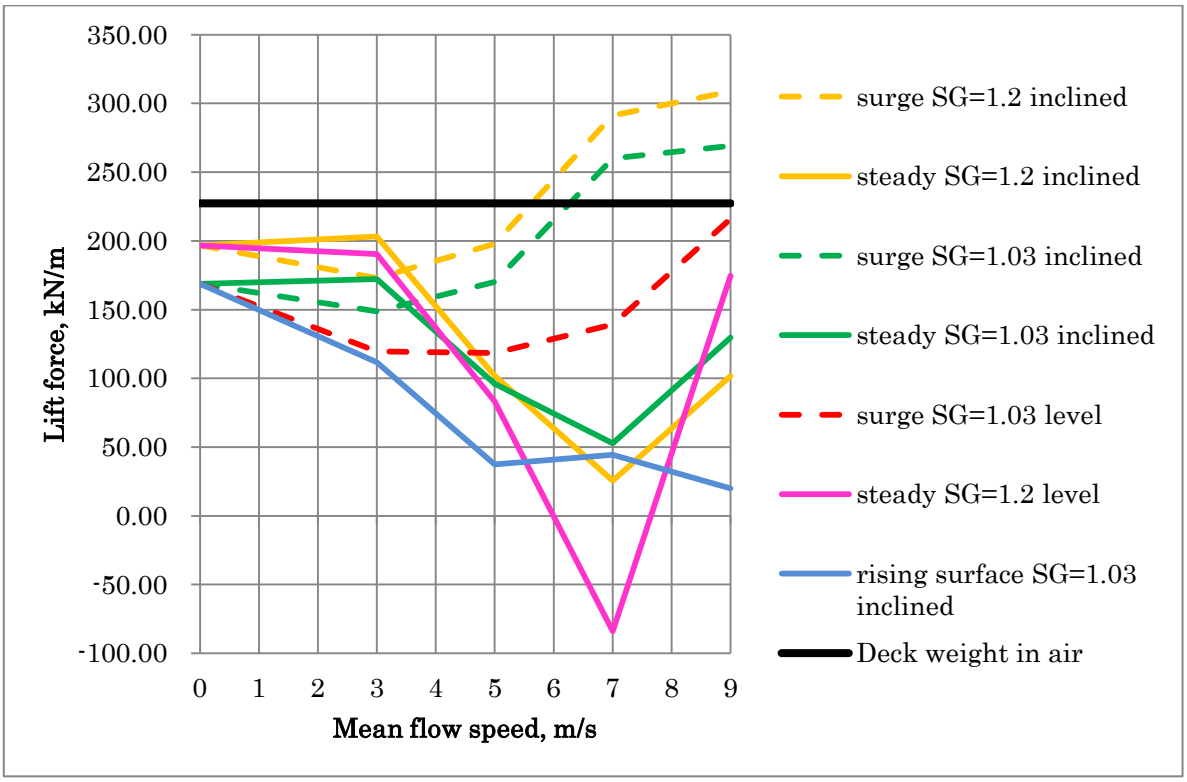

Figure 13. Summary of maximum (in time) lift force on the bridge deck in each scenario. The thick black line indicates the weight of the bridge. Liftoff of the deck can occur when lift force exceeds the bridge weight.

Another item of importance to the overturning moment is flow density. For the surge cases, the difference in moment between the SG=1.03 case and the SG=1.2 case is as large as approximately 250 kNm/m. This is the same order as the static contribution of air trapped between girders. For the steady-flow cases, deck failure at low speeds does not occur for the SG=1.03 case, indicating that entrained sediment might have been essential for causing deck failure at Utatsu.

CONCLUSIONS

Smoothly rising water surface, steady-flow, and surge simulations were carried out to investigate the cause of deck failure of a typical bridge of the size and shape of the Utatsu Bridge during the 2011 Tohoku Tsunami. Simulation results indicate that surge, where present, could cause deck failure. In lieu of surge, at subcritical flow speeds a smoothly rising water surface would not cause bridge deck failure, because accelerated flow under the bridge deck causes a negative lift. However, once the flow significantly submerges the bridge deck so that flow accelerates as much over the deck as it does under the deck, vortex shedding and free-surface fluctuations can cause the deck to overturn.

At Utatsu, surge was not evident in the video. The bridge appeared to be submerged by three to four meters, and the flow speed appeared to be between 3 m/s and 5 m/s based on a fishing boat seen drifting over the bridge site. Furthermore, at this high water level, the water surface over the bridge site experienced only small fluctuations. These conditions are similar to those modeled in the 3 m/s steady flow case. The model only shows deck overturning for the case of a sediment-laden flow, but whether this was the case at Utatsu could not be determined from the video. Also undetermined is

whether the seawall located landward of the Utatsu bridge could have contributed to deck failure; this will be the subject of further investigation.

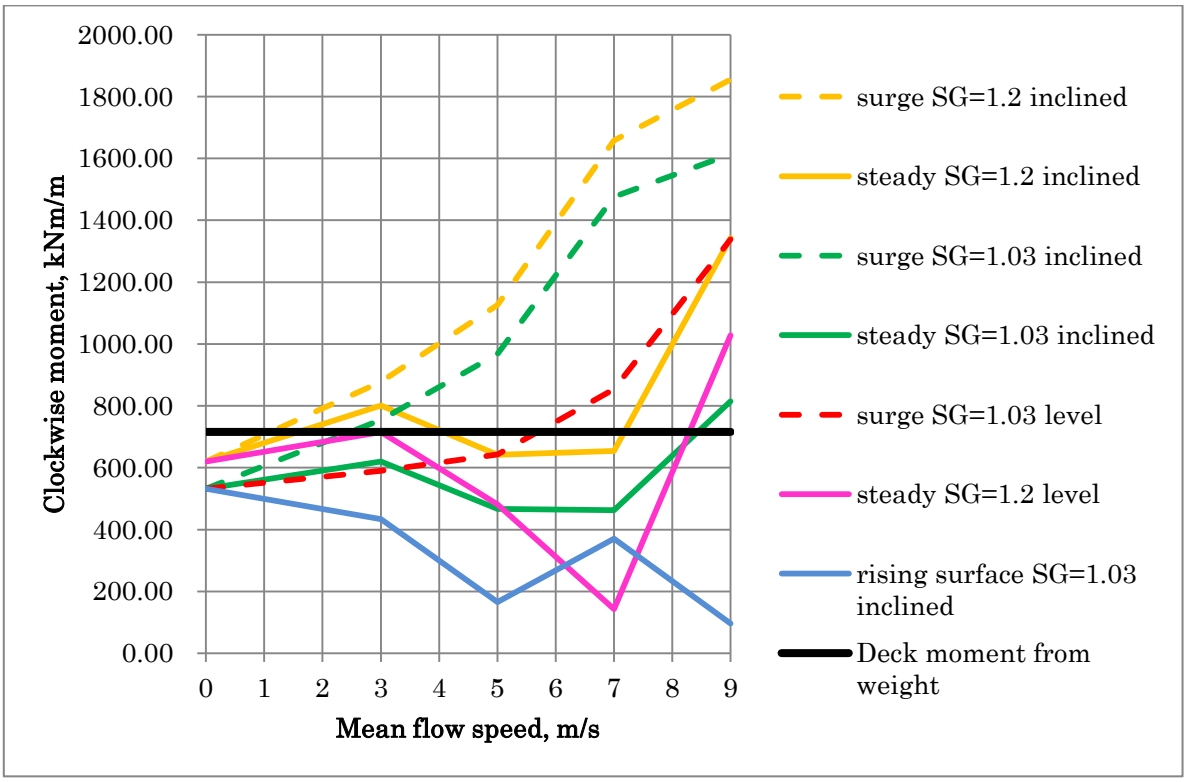

Figure 14. Summary of maximum (in time) overturning moment (upward on the seaward edge of the bridge deck) about the landward edge of the landward-most girder, for each scenario. The thick black line indicates the counterclockwise moment due to the weight of the bridge deck. Overturning of the deck can occur when the clockwise moment due to fluid forces exceeds the counterclockwise moment due to bridge deck weight.

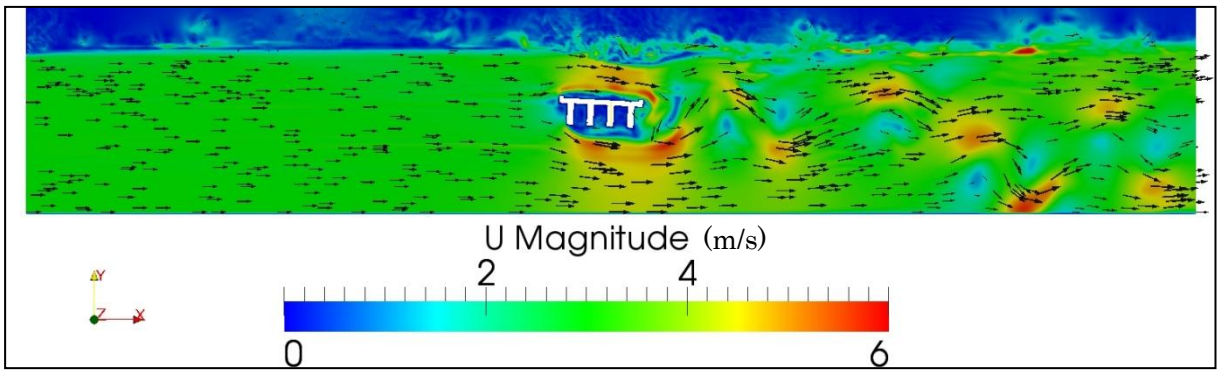

Figure 15. Flow velocity magnitude and vectors at t=29 sec for the bridge subject to steady flow of speed 3 m/s and depth 15 m. Water density is 1200 kg/m^3.

For a bridge subjected to either a subcritical steady flow or a surge, the combination of two actions could prevent deck failure:

1. Construction of an escape path for trapped air that is large enough to allow air to evacuate quickly during the approach of a surge or flood, and
2. Replacement of the inclined deck with a level deck.

In addition to this, UPD's must be strong enough to withstand the drag force of the flood (Figure 16).

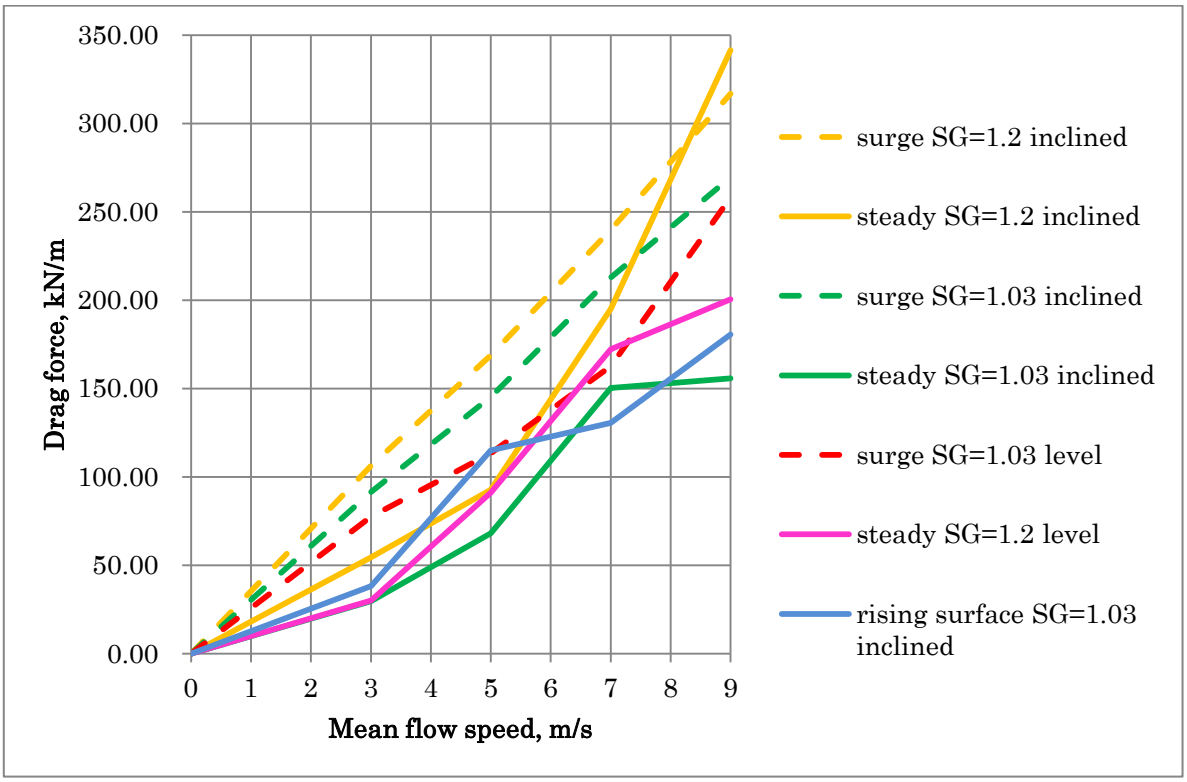

Figure 16. Summary of maximum (in time) drag force on bridge deck in each scenario.

ACKNOWLEDGMENTS

The authors are grateful to Mr. Katsuya Oikawa and the citizens of Minamisanriku for providing video of the tsunami and first-hand accounts of the event.

REFERENCES

Applied Technology Council. (2008). "Guidelines for Design of Structures for Vertical Evacuation from Tsunamis." *Report FEMA P646 of the Federal Emergency Management Administration.*

Chen, G., Emitt, C.W. III, Hoffman, D., Luna, R., and Sevi, A. (2005). "Analysis of the Interstate 10 Twin Bridge's Collapse During Hurricane Katrina." *Science and the Storms: the USGS Response to the Hurricanes of 2005*, pp 35-42.

Kerenyi, K., Sofu, T., and Guo, J. (2009). "Hydrodynamic Forces on Inundated Bridge Decks." *Report No. FHWA-HRT-09-028 of the Federal Highway Administration.*

Kundu, P.K. (1990). *Fluid Mechanics*. Academic Press. San Diego. p 323.

OpenFOAM (2011). *OpenFOAM version 2.1.0 User Guide*. www.openfoam.org.

Patil, S., Kostic, M., and Majumdar, P. (2009). "Computational Fluid Dynamics Simulation of Open-Channel Flows Over Bridge-Decks Under Various Flooding Conditions." *Proceedings of the 6th WSEAS International Conference on Fluid Mechanics (FLUIDS'09)*, pp 114-120.